Neohesperidin Mitigates High-Fat Diet Induced Colitis *In vivo* by Modulating Gut Microbiota and Enhancing SCFAs Synthesis

Kun Lu , Sijie Shan , Yanling Zeng , Guliang Yang *

Posted Date: 5 December 2024

doi: 10.20944/preprints202412.0473.v1

Keywords: neohesperidin; intestinal microbiota; SCFAs; JAK2/STAT3 pathway; intestinal mucosa

Article

Neohesperidin Mitigates High-Fat Diet Induced Colitis *In vivo* by Modulating Gut Microbiota and Enhancing SCFAs Synthesis

Kun Lu [1,†], Sijie Shan [1,†], Yanling Zeng [2] and Guliang Yang [1,*]

[1] National Engineering Laboratory for Rice and By-Products Processing, Food Science and Engineering College, Central South University of Forestry and Technology, Changsha 410004, China
[2] Key Laboratory of Cultivation and Protection for Non-Wood Forest Trees, Ministry of Education, Central South University of Forestry and Technology, Changsha 410004, China
* Correspondence: 469436773@qq.com; +86-731-85658893
† These authors contributed equally to this work, both of them are the first author of the paper.

Abstract: Previous research has consistently shown that high-fat diet (HFD) consumption can lead to the development of colonic inflammation. Neohesperidin (NHP), a naturally occurring flavanone glycoside in citrus fruits, has anti-inflammatory properties. However, the efficacy and mechanism of NHP in countering prolonged HFD-induced inflammation remains unclear. In this study, rats on HFD were intragastric administered (i.g.) with NHP for 12 consecutive weeks. Results indicated that this natural compound is effective in reducing colorectal inflammation at doses of 40-80 mg/kg body weight by i.g. administration, with significant decreases in inflammation markers such as TNF-α and IL-1β levels. It also improved intestinal mucosal tissue integrity and reduced HFD-stimulated colorectal inflammation via the JAK2/STAT3 pathway. Furthermore, intestinal microbiota sequencing results showed that NHP intervention significantly downregulated the Firmicutes/Bacteroidetes ratio. This ratio is closely related to the preventive role in the context of glycolipid metabolism disorder. Compared with fecal cultures of rats from the HFD group, after 48 h *in vitro* fermentation, those from the NHP group had distinct microbiota composition and notably higher concentrations of SCFAs. Collectively, these observations suggest that NHP's biological activities in downregulating HFD-induced colorectal inflammation are achieved by regulating intestinal flora and promoting SCFAs formation.

Keywords: neohesperidin; intestinal microbiota; SCFAs; JAK2/STAT3 pathway; intestinal mucosa

1. Introduction

Existing research reveals that individuals who consume high-fat diets (HFD) for extended periods of time often experience excessive accumulation of fat. This process is often accompanied by dysregulation of the gut microbiota and increased levels of inflammation. Gut microbiota is a symbiotic ecosystem consisting of the host and a large number of gut microbes. The study of the impact of gut microbiome on chronic conditions such as obesity associated with HFD consumption has recently emerged as an area of significant scientific interest [2]. Studies have confirmed that gut microbiota is closely linked to dietary-induced obesity [3]. Feeding germ-free mice a HFD led to distinct alterations in glucose loading tolerance, insulin sensitivity, and obesity compared to their normally fed counterparts. This highlights the significant impact of diet on gut microbiota [4]. Transplanting the gut microbiota of obese mice into the guts of normal mice led to obesity in these previously healthy mice [5]. In addition, numerous studies on gut microbiota composition in obese individuals and gut microbiota transplantation experiments have also demonstrated the crucial role of the gut microbiota in the pathogenesis of obesity [6].

With advances in gut microbiota research, the notion that gut microbiota serves as a target for dietary effects on host health has gained widespread acceptance [7]. HFD imposes potential perturbation on the native microbial population and its function in the gut. The composition and function of the gut microbiota is an intricate biological mechanism that can significantly impact

 doi:10.20944/preprints202412.0473.v1

various host biological processes, including immune and inflammatory responses. The gut microbiome is capable of producing and metabolizing various compounds, which can affect intestinal barrier function and various signaling pathways. These changes can subsequently affect the host's metabolic equilibrium and overall health status [8]. The intestinal barrier exhibits selective permeability, which prevents the invasion of pathogenic microorganisms, toxins, and other harmful substances. It also ensures the normal absorption of nutrients and electrolytes. Therefore, the integrity of the intestinal barrier directly affects gut homeostasis [9]. Once this balance is disrupted, it can affect intestinal mucosa barrier function [10]. Current research has confirmed that Mucin 2 (MUC2) is the predominant component of mucins. This protein has the activity of inhibiting the activation of downstream inflammatory responses mediated by activating IL-6/JAK/STAT3 signaling cascade [11,12]. Therefore, MUC2 is crucial for maintaining the integrity of the intestinal mucosal barrier [13].

In vivo, specific gut microbiota can convert dietary fiber into short-chain fatty acids (SCFAs), such as acetic acid, propionic acid, butyric acid, and others. These SCFAs are of great significance in maintaining gut health. They also play an essential role in regulating the immune system and exerting an influence on energy metabolism [14], promoting intestinal peristalsis, and enhancing intestinal barrier function [15]. Chronic inflammation causes gut dysbiosis characterized by decreased probiotics and increased harmful bacteria. There is a decrease in the proportion of beneficial bacteria and an increase in the abundance of harmful bacteria. Concurrently, the level of SCFAs is significantly reduced [14].

Citrus flavonoids can stimulate the proliferation of beneficial bacteria, such as *Bifidobacterium* and *Lactobacillus*, which are able to ferment dietary fiber efficiently to produce SCFAs [16]. This category of compounds also exerts an inhibitory effect on the growth of harmful gut microbiota. Therefore, it helps maintain the balance of the gut microbiota community and facilitates the formation of SCFAs [17]. Neohesperidin (NHP) exerts its anti - inflammatory effect by inhibiting the activation of pro - inflammatory cytokines and modulating immune cell functions. Its antioxidant property is attributed to scavenging free radicals and reducing oxidative stress [18]. Scientific researches [19,20] have verified that NHP is effective in alleviating the symptoms of ulcerative colitis induced by the administration of sodium dextran sulfate (DSS), and this activity is closely related to its ability to modulate gut microbiota composition. However, the precise mechanism by which it exerts its effectiveness against colitis, especially its influence on the gut microbiota, remains to be elucidated. This study aims to comprehensively investigate the mechanism by which NHP regulates gut microbiota and SCFAs synthesis to fill these knowledge gaps and provide new insights into the treatment of HFD-induced colitis.

This study evaluated the impact of intragastrically administered NHP on the biodiversity and predominance of the gastrointestinal microbiota as well as inflammation in rats on a HFD for 12 consecutive weeks. In addition, the molecular mechanism by which NHP prevents HFD-induced colorectal inflammation was investigated, thus laying a theoretical foundation for the efficient utilization of NHP.

2. Results and Discussion

2.1. NHP Improved Lipid Metabolism Disorders in HFD Rats

Fig. 1A indicated that HFD rats exhibited markedly heavier body weights (601.4 g vs 684.8 g, $p < 0.05$) compared to Ctrl rats. NHP treatment slightly reduced body weights (NHP40: 660.1 g, NHP80: 655.0 g). Although food intake remained constant, it suggests that NHP's effect on obesity is unrelated to reduced intake (Fig. 1B). Figs. 1C and 1D revealed significant elevations in serum ALT and AST activities ($p < 0.01$) in HFD rats compared to Ctrl (ALT: HFD vs Ctrl, $p < 0.01$; AST: HFD vs Ctrl, $p < 0.01$). Interestingly, NHP40 and NHP80 rats showed decreased serum ALT and AST activities ($p < 0.05$ or $p < 0.01$), indicating improved liver function. Figs. 1E-1H showed substantial increases in serum TC, TG, and LDL-C for HFD rats ($p < 0.05$ or $p < 0.01$), but decreased HDL-C levels ($p < 0.01$). NHP treatment effectively regulated these markers: serum TC, TG, and LDL-C levels were reduced ($p < 0.05$ or $p < 0.01$), and HDL-C levels were elevated ($p < 0.05$). In conclusion, these findings suggest that chronic HFD induced lipid metabolism disorders in rats, which were effectively managed by NHP intervention.

 doi:10.20944/preprints202412.0473.v1

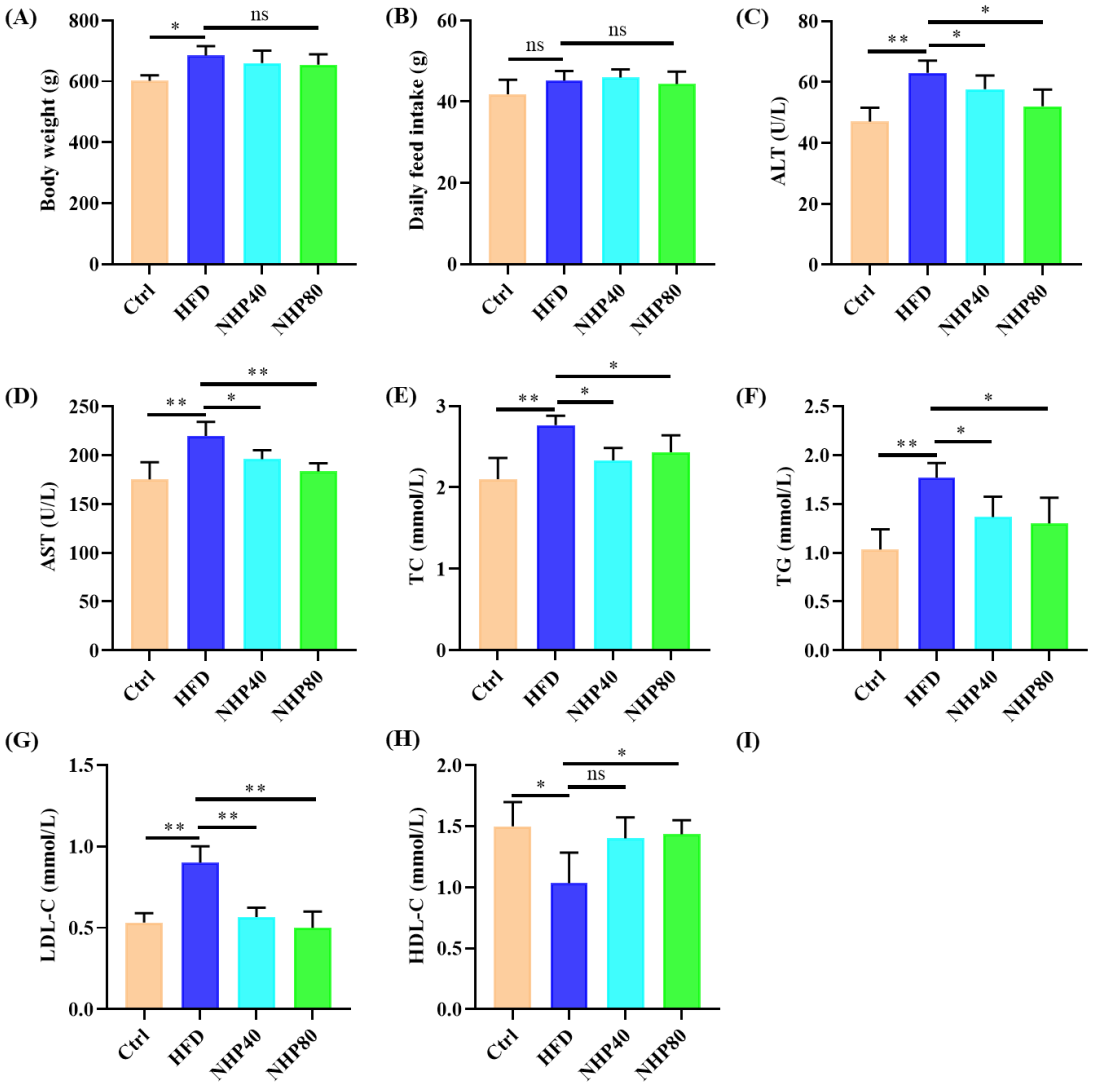

Figure 1. NHP Mitigates Obesity Development in HFD Rats. (A) Body weight at 12 weeks post-NHP treatment. (B) Daily food consumption. Serum parameters include (C) ALT, (D) AST, (E) TC, (F) TG, (G) LDL-C, and (H) HDL-C. Data are presented as mean ± SD (n = 3. *indicates significance, *$p < 0.05$, **$p < 0.01$. ns: no significant difference. hereinafter the same).

2.2. NHP Improved Pathological Ileum Injury

H&E staining (Figure 2A) demonstrated that HFD induced abnormal proliferation of goblet cells, damage to lamina propria, and villous atrophy, thereby disrupting submucosal architecture. In contrast, NHP significantly altered these growth patterns. Immunohistochemical (IHC) staining revealed that HFD decreased levels of ZO-1 (Figure 2B, D) and Occludin (Figure 2C, E) in the ileum. NHP enriched the expression of ZO-1 (0.149 in Ctrl group, 0.049 in HFD group, 0.095 in NHP40 group, 0.067 in NHP80 group) and Occludin (0.298 in Ctrl group, 0.134 in HFD group, 0.288 in NHP40 group, 0.276 in NHP80 group), indicating enhanced intestinal tight junctions. These proteins significantly regulated cell polarity, apical domain development, and impacted crucial cellular activities including proliferation, differentiation, and migration [21]. Impairment of tight junctions might have indicated severe gastrointestinal pathologies [22]. Prolonged exposure to HFD elevates oxidative stress, leading to a lack of tight junctions and significantly affecting the integrity of the gut epithelial barrier.

 doi:10.20944/preprints202412.0473.v1

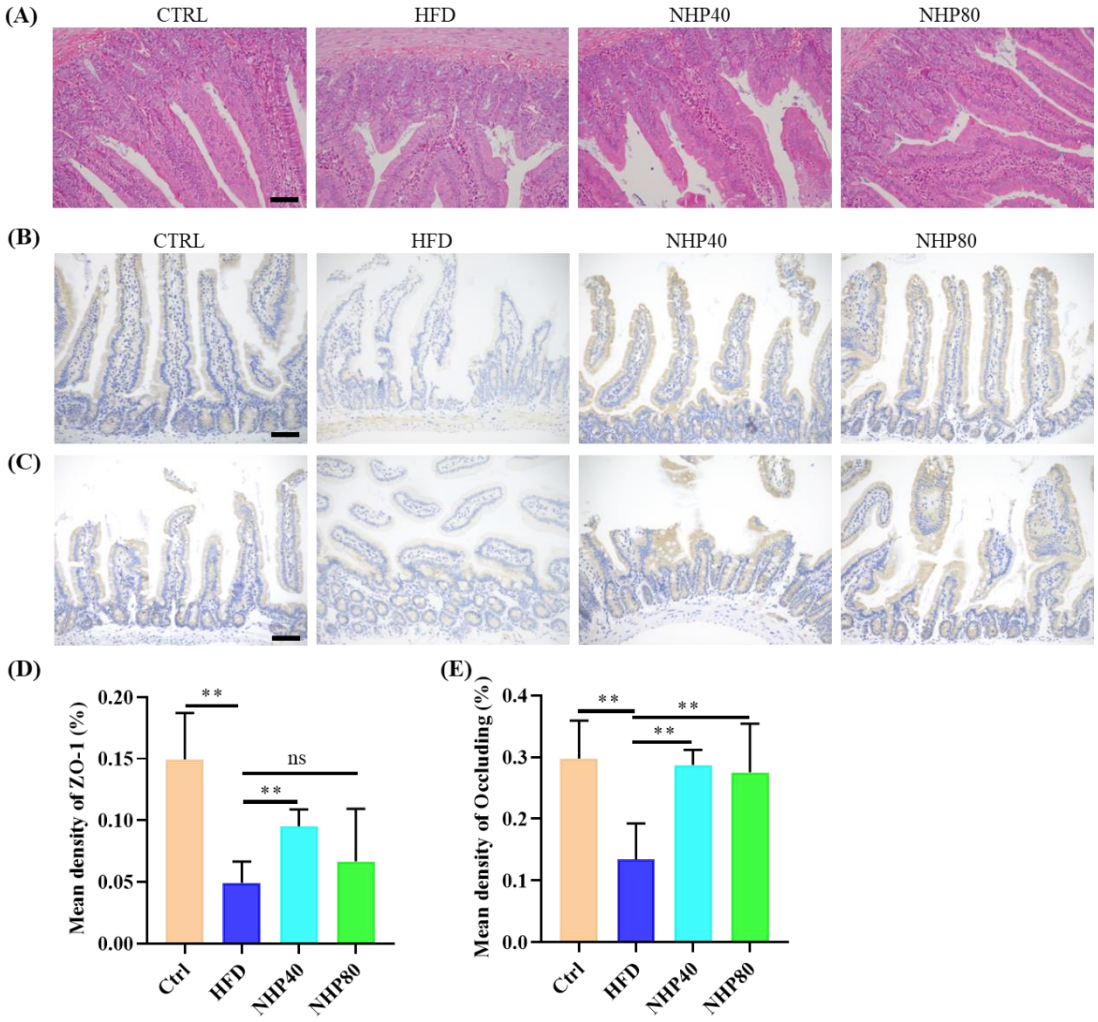

Figure 2. HE and IHC Examination of Intestinal Tissue. (A) HE staining of intestinal tissues. (B) IHC of ZO-1 and (D) its quantification. (C) IHC of Occludin and (E) its quantification (200×). The scale bar = 200 μm.

2.3. NHP Mitigated HFD-Induced Inflammation

Figures 3A–3C illustrate the potent anti-inflammatory efficacy of NHP, as evidenced by a significant reduction in the levels of TNF-α, IL-1β, and IL-6 ($p < 0.01$). Correspondingly, Figures 3D–3H reveal an amplification of JAK2/STAT3 signaling in the HFD cohort compared to Ctrl ($p < 0.01$). Elevated circulating levels of TNF-α, IL-1β, and IL-6 are indicative of inflammation [23]. These findings suggest that NHP treatment attenuated HFD-induced inflammation. Dose-dependent suppression of p-JAK2 and p-STAT3 proteins by NHP was observed in **Figures 3**D-3H. Specifically, p-JAK2 protein expression decreased to 2.09-fold in NHP80 and 1.48-fold in NHP40, respectively, from 2.79-fold in the HFD group. Similarly, p-STAT3 protein expression declined to 2.60-fold in NHP80 and 1.75-fold in NHP40, respectively, from 3.54-fold in the HFD group. In conclusion, NHP effectively counteracted HFD-induced inflammation by activating the JAK2/STAT3 pathway.

 doi:10.20944/preprints202412.0473.v1

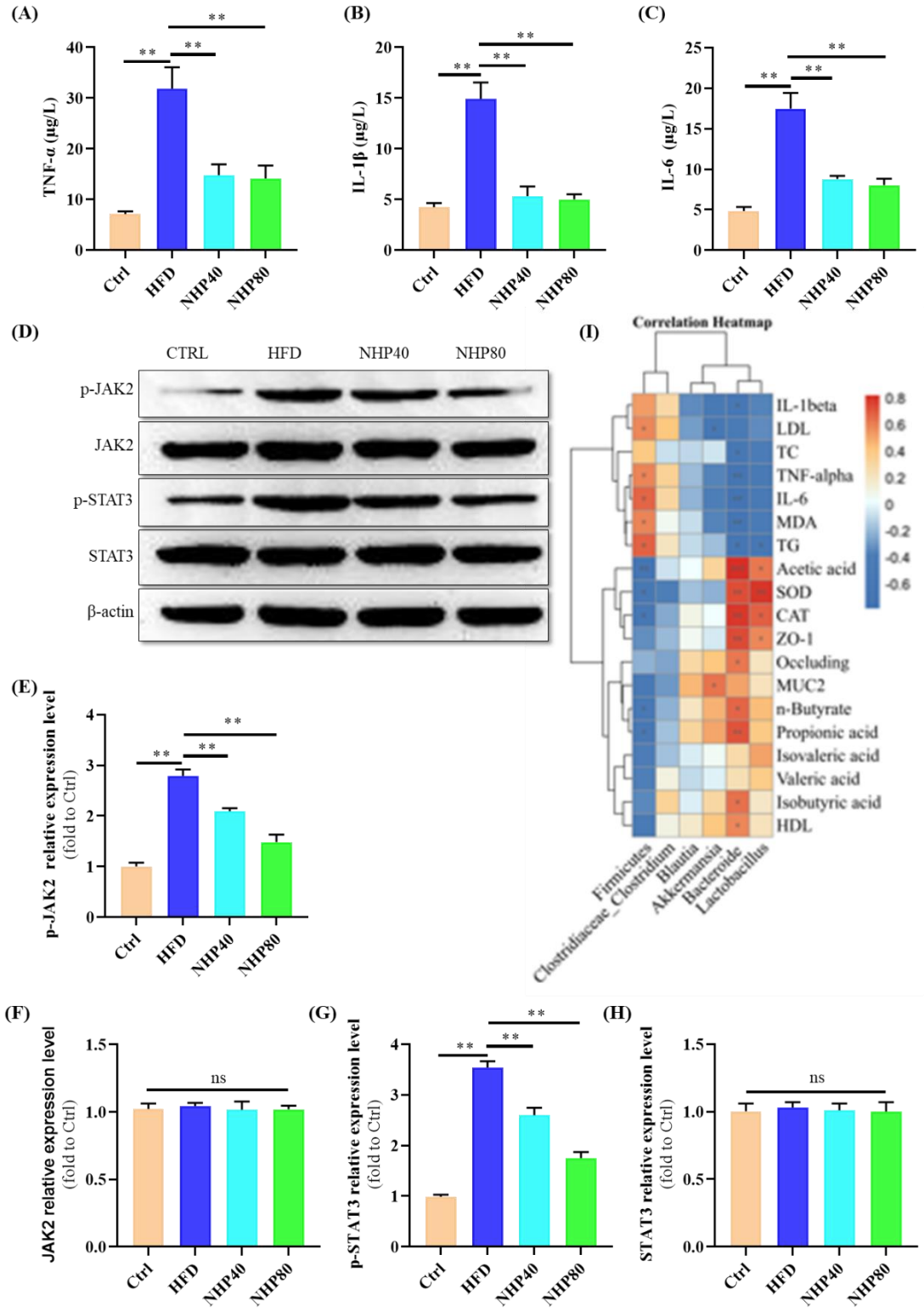

Figure 3. The level of tissue inflammation. The relative expression levels of (A) TNF-α, (B) IL-1β and (C) IL-6. (D) Western blot results. (E-H) quantification results and (I) Pearson correlation analysis results.

2.4. NHP Maintained the Integrity of Colonic Mucosa

In addition to its beneficial effects on lipid metabolism and inflammation, NHP also exhibited a significant role in maintaining the integrity of the colonic mucosa. Figure 4A showed a significant reduction in AB-PAS-stained areas during chronic HFD intake. NHP treatment counteracted HFD-induced depletion of goblet cells. Western blot analysis indicated a significant decrease in MUC2 protein expression in ileal tissue from the HFD group (Figures 4B-C), reaching only 0.33 times the

 doi:10.20944/preprints202412.0473.v1

Ctrl group. Interestingly, NHP significantly increased the relative expression of this protein ($p < 0.01$). AB-PAS staining is a widely used technique to detect intestinal and gastric mucous substances. In this method, glycogen and neutral mucous substances stain red, while acidic substances stain blue. The intestinal mucosal layer is vital in forming the mucosal barrier, with MUC2 being the primary mucin component. Thus, NHP mitigated HFD-induced colon mucosa damage by reducing inflammation.

2.5. NHP Elevated the Level of SCFAs

In Figure 4D, stool SCFAs data indicated a significant decline in acetic acid, n-butyrate, and propionate levels among individuals on HFD. After supplementation with NHP, this trend was reversed, suggesting a functional correlation. Acetic, propionic, and butyric acids, which are produced from carbohydrate digestion by gut bacteria, will be rapidly utilized within humans [24]. Acetic acid has been found to enhance glucose tolerance and insulin release in overweight animals [25]. Butyric acid, which is essential for colon epithelial energy production, is beneficial in the fight against diabetes and insulin resistance [26]. Propionic acid, an essential gut metabolite, confers benefits to fat cells through anti-inflammatory effects, promoting adipocyte glucose utilization and lipogenesis [27]. Consequently, we suggest that NHP influenced SCFAs through gut microbiota regulation.

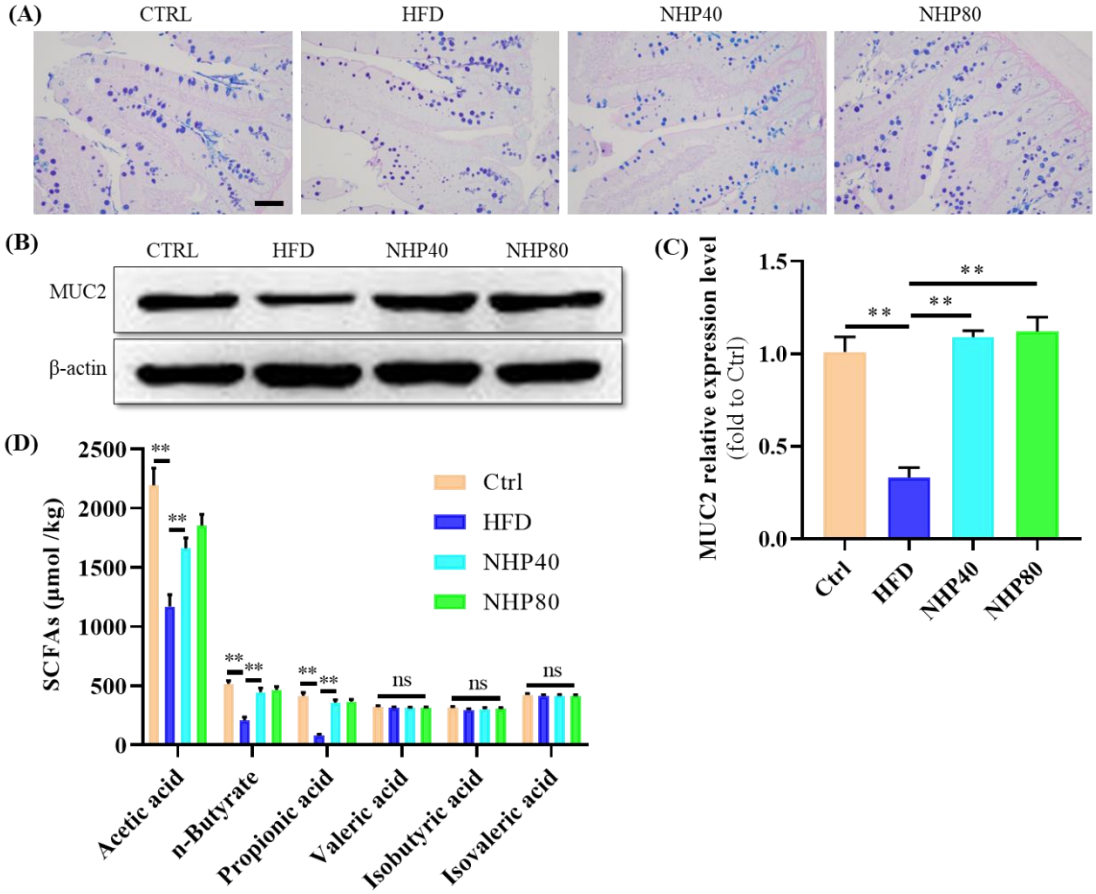

Figure 4. Analysis of AP-BAS staining, Western blot and SCFAs content. (A) AP-BAS staining results, (B) Western blot results and (C) quantification results, (D) content of SCFAs.

2.6. NHP Regulated Intestinal Flora Diversity

PCA analysis (Figure 5A) revealed the distinct positioning of Ctrl in the lower left corner, demonstrating a significant impact of HFD on gut flora. The NHP40 and NHP80 groups exhibited unique features from the HFD and Ctrl groups, suggesting partial restoration of HFD-induced alterations by NHP. Figures 5B and 5C illustrated a decrease in species richness and evenness in rats fed HFD compared to Ctrl. However, NHP treatment did not significantly alter these parameters. As

 doi:10.20944/preprints202412.0473.v1

depicted in Figure 5D, NHP affected gut population composition. Shared amplicon sequence variants (ASVs) of 514, 337, and 473 were observed for Ctrl and HFD, Ctrl and NHP40, and Ctrl and NHP80, indicating NHP-induced shifts in gut microbiota composition. The Chao1 index represents species richness, and the Shannon index measures species evenness. These findings suggest that NHP treatment altered the composition of gut bacteria in experimental animals.

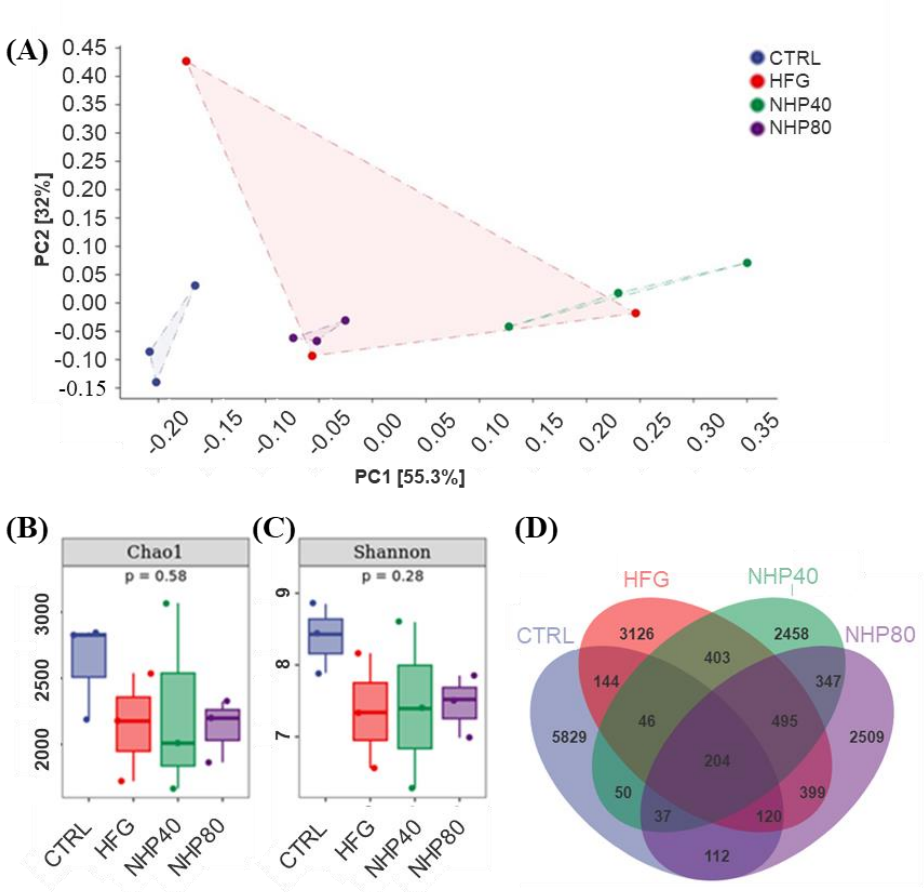

Figure 5. 16S rDNA Sequencing of Bacterial Communities. (A) PCA, (B) the Chao1 index, (C) the Shannon diversity index, and (D) ASV Venn diagram.

2.7. NHP Modulated the Overall Structure and Composition of Gut Microbiota

At the genus level, the gut microbiota consisted mainly of genera including *Blautia*, *Lactobacillus*, *Akkermansia*, *Oscillospira*, *Allobaculum*, *Bacteroides*, *Clostridium*, *Phascolarctobacterium*, *Turicibacter*, and *SMB53* (Figure 6A). Compared to Ctrl, the proportion of Bacteroidetes decreased significantly in HFD ($p < 0.01$) (Figure 6B), while Firmicutes increased substantially ($p < 0.05$) (Figure 6C). This indicates that HFD treatment notably enhanced the Firmicutes/Bacteroidetes (F/B) ratio. Administration of NHP resulted in a significant increase in Bacteroidetes and a reduction in Firmicutes proportions. Previous studies have shown that an elevated F/B ratio in the HFD group is associated with nutrient accumulation, adipogenesis, and fat storage [28]. Thus, the reduced F/B ratio may be related to NHP's protective role against glycolipid metabolism disorders. As shown in Figure 6D, *Clostridium* levels remained unchanged among the groups. *Lactobacillus*, which produces lactic acid and plays a crucial role in maintaining the intestinal mucosal barrier, regulating the immune system, and promoting digestion and absorption [29], exhibited a significant increase in abundance in the NHP80 group ($p < 0.05$) (Figure 6E). Research by Hosimi et al. [30] has shown that higher levels of *Blautia* suggest a smaller visceral fat area. *In vitro* and *in vivo* experiments have also confirmed *Blautia*'s ability to reduce BW, inflammation, and insulin resistance [31]. Consequently, this bacterium has emerged as a key obesity-related gut bacterium [30]. In this study, NHP treatment significantly increased *Blautia* abundance (Figure 6F). A deficiency or reduction in *Akkermansia* is linked to obesity and diabetes. The increase in beneficial bacteria such as Blautia and Akkermansia may contribute to improved lipid

 doi:10.20944/preprints202412.0473.v1

metabolism through mechanisms such as enhanced bile acid metabolism and reduced inflammation - induced insulin resistance. Future studies are needed to further elucidate the detailed molecular pathways. It stores mucin, which is beneficial for maintaining the intestinal barrier [32]. Fortunately, after NHP treatment, the level of this bacterium increased significantly (Figure 6G). Functional microbiota prediction (Figure 6H) revealed that the differential gut microbiota focused primarily on biosynthesis, particularly amine, polyamine, fatty acid, nucleotide, and cofactor biosynthesis. These findings suggest that NHP effectively alleviates elevated HFD-induced inflammation and potentially preserves the structural integrity of intestinal epithelial tissue by modifying the gut microbiota.

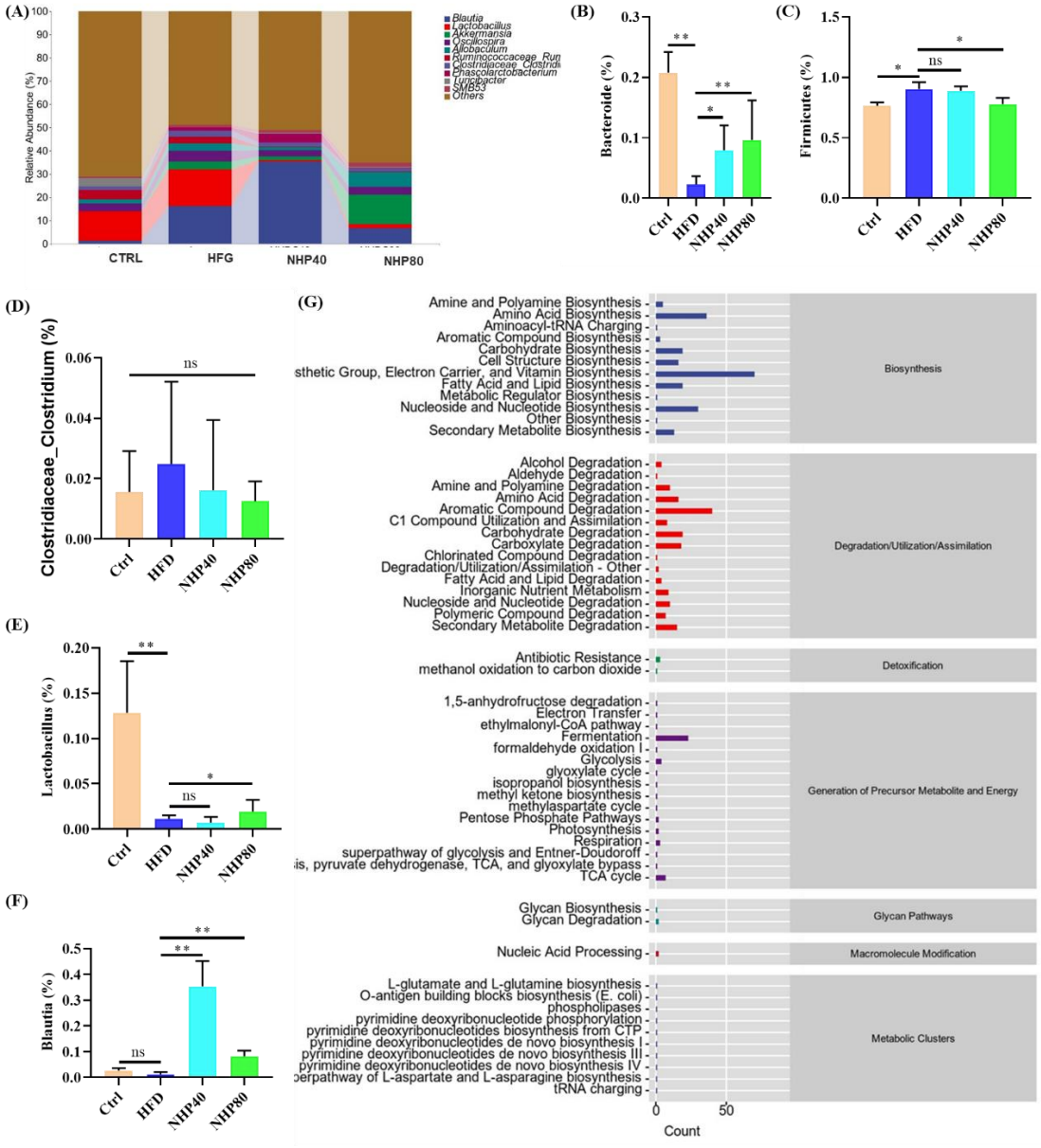

Figure 6. Bacterial Composition and Abundance in the Gut Microbiota. (A) Genus-level composition. Relative abundance of (B) *Bacteroide*, (C) Firmicutes, (D) *Clostridium*, (E) *Lactobacillus*, (F) *Blautia*, and (G) *Akkermansia*. (H) KEGG metabolic pathway comparison.

2.8. In vitro Fermentation Results

2.8.1. Fermentation pH Fluctuation

As shown in Figure 7A, the pH values of both FFM and NFM decreased gradually over the 0-48 h fermentation period. Specifically, the pH value of FFM dropped from 6.27 at 0 h to 5.87 at 48 h, while the pH value of NFM decreased from 6.30 to 5.57. Research [33] has shown that an appropriate

 doi:10.20944/preprints202412.0473.v1

decrease in the pH of the gut lumen can provide beneficial conditions for the growth of beneficial colonic microbiota and inhibit the growth of harmful microorganisms.

2.8.2. Fermentation Gas Production

As illustrated in Fig. 7B, gas production increased steadily as fermentation progressed. The FFM group produced 8.5 mL of gas over 48 h. FFM gas production was 6.0 mL. Carbohydrates and proteins will be hydrolyzed by colonic flora, giving rise to gases such as carbon dioxide, hydrogen, and methane. Although certain gases facilitate intestinal peristalsis, excessive gas can lead to adverse consequences such as abdominal distension and appetite suppression [34].

2.8.3. Microbiota Composition and SCFAs Production

Quantification of bacterial populations in the fermentation broth revealed an increase in total bacteria as well as abundance of *Prevotella*, *Bacteroides*, *Lactobacillus*, and *Blautia*. In contrast, *Clostridium* populations decreased significantly in the FFM group (Figure 7C). These bacterial genera are well-known producers of SCFAs [35]. *Prevotella*, for example, contributes significantly to carbohydrate degradation and produces acetic and propionic acids. *Bacteroides* ferments dietary fiber to produce acetic, propionic, and butyric acids. *Lactobacillus* produces lactic acid, which is further converted into SCFAs by other gut bacteria [35-37]. After 48 h of fermentation, significant differences in specific SCFAs were observed between the two groups (Figure 7D). Specifically, the levels of acetic acid, n-butyrate, propionic acid, and isobutyric acid in the NFM group were 1300, 231, 373, and 314 μmol/L respectively, which were significantly higher than those in the FFM group (945, 197, 308, and 282 μmol/L). In conclusion, NHP treatment increased the abundance of bacteria capable of producing SCFAs in the feces of experimental rats. However, this study has certain limitations. For example, the long - term effects of NHP treatment need to be further investigated.

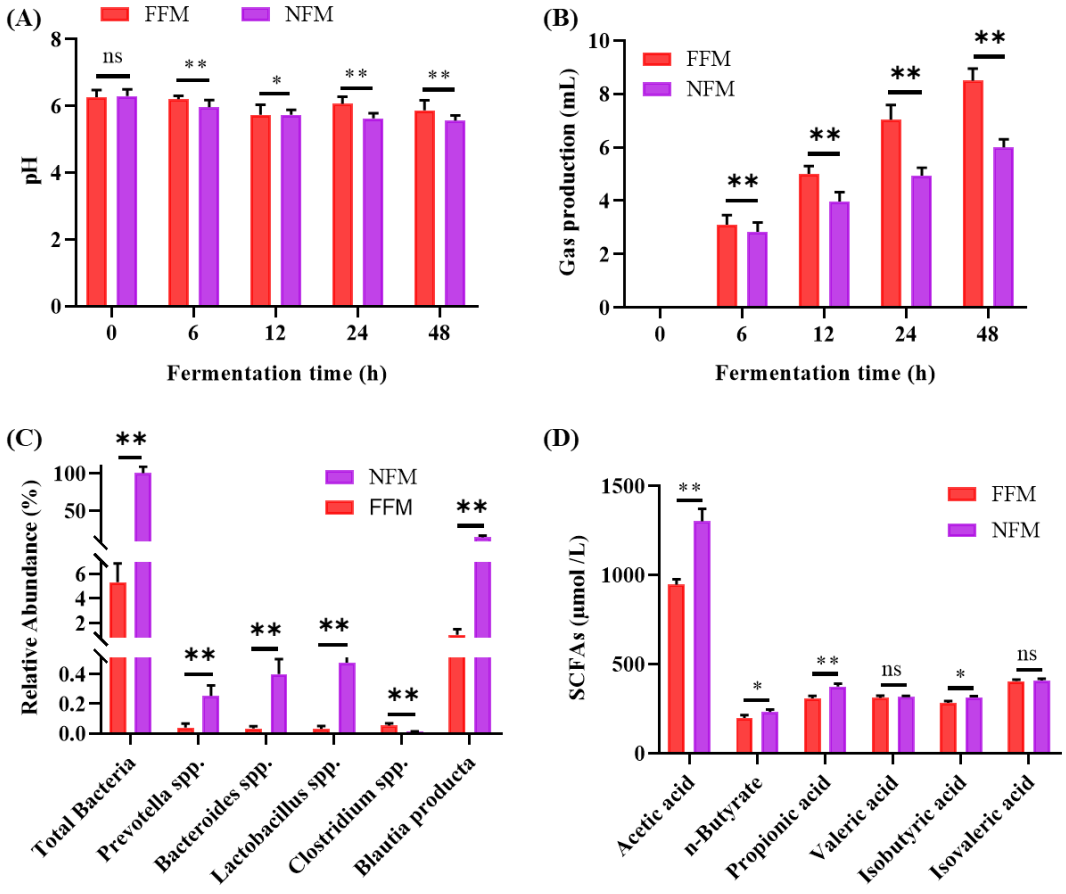

Figure 7. *In vitro* fermentation culture results. (A) pH change, (B) gas production, (C) SCFAs concentrations, and (D) intestinal microbiota composition in fermentation cultures.

 doi:10.20944/preprints202412.0473.v1

3. Materials and Methods

3.1. Experimental Materials

NHP was acquired from Kang Biotech (Lianyuan, Hunan, China). DNeasy PowerSoil Kit (Cat #12888-100) was purchased from Qiagen (Hilden, Germany). Q5® High-Fidelity DNA Polymerase (Cat #M0491L) was purchased from NEB (Ipswich, MA, USA). The double-stranded DNA quantitative assay kit (Cat #P7589) was procured from Invitrogen, located in Carlsbad, CA, USA. Agencourt AMPure XP (Cat #A63881) was purchased from Beckman Coulter (Brea, CA, USA). NovaSeq 6000 SP Reagent Kit (Cat #20028402) was purchased from Illumina (San Diego, CA, USA). AXYGEN DNA Gel Recovery Kit (Cat #AP-GX-50G) was purchased from Axygen biosciences (Union City, CA, USA). Acetic acid, propionic acid, n-butyrate, valeric acid, isobutyric acid, and isovaleric acid were all procured from Sigma-Aldrich, located in St. Louis, MO, USA).

3.2. Experimental Animals and Treatments

In this study, subject animals were Sprague-Dawley (SD) males aged 5-6 w and 180-220 g, SPF-qualified, from SJA, in Changsha, Hunan, China. They were housed in a SPF environmental condition, and the incubation ambient conditions were maintained at a temperature range of 20 to 26°C, humidity ranging from 40% to 70%, and a fixed 12-hour light/12-hour dark cycle. Throughout the experimental period, all rodents received unrestricted access to water and food. Laboratory animal experiments were carried out at the Institute of Laboratory Animal Research (Hunan University of Chinese Medicine). Laboratory rodent diets, including high-fat and basic types, were purchased from BKF Co., Ltd. (Beijing, China). Following one-week adaptation, rats were divided into four equal-sized groups, with eight animals in each group, including blank control group (Ctrl, fed basic laboratory rodent diet), HFD model group (HFD, high-fat laboratory rodent diet), 40 mg/kg body weight (BW) NHP treatment group (NHP40, fed HFD and intragastric administration of 40 mg NHP/kg BW per day), and 80 mg/kg BW NHP treatment group (NHP80, fed HFD and intragastric administration of 80 mg NHP/kg BW per day). The doses of 40 mg/kg and 80 mg/kg were selected based on previous studies and preliminary experiments in our laboratory, which showed significant effects on relevant indicators. For administration, NHP was reintegrated into a 0.5% sodium carboxymethylcellulose (CMC-Na) environment. An equivalent dose of CMC-Na gel was provided daily to both Ctrl and HFD NHP-free groups over a 12-week period. Biweekly BW and weekly diet intake assessments were performed. After treatment, the animals were humanely euthanized with chloral hydrate, along with intestinal contents, blood serums, and liver collections.

3.3. Colorectal Histopathological Examination

Colorectal tissue was subjected to H&E or AB-PAS staining to display histopathological characteristics. Specifically, colon segments preserved in formalin or Carnoy's solution were subjected to H&E or AB-PAS staining, respectively. After a 24-hour fixation period, colonic tissue was dehydrated, paraffin-embedded, and segmented into thin slices. Afterwards, they were treated with H&E or AB-PAS. Pathological assessments were carried out using an Olympus BH2 microscope (Hino, Japan) at a magnification of 200×.

3.4. Immunohistochemical Detection

After deparaffinization, tissue sections were accurately adhered to gelatinized slide chambers. These slides were then subjected to initial immune staining with anti-ZO-1 (Cat# 21773-1-AP), anti-Occludin (Cat# 13409-1-AP), or anti-MUC2 (Cat# 27675-1-AP) from Proteintech, Wuhan, China. Rinse with PBS was performed prior to application of HRP-tagged secondary antibody (Abcam's Cat# ab205718, USA). Subsequently, DAB staining (Sigma-Aldrich) and hematoxylin counterstaining were carried out to facilitate the assessment of immunoreactivity using the H-score methodology. In this methodology, scores of 1, 2, and 3 were assigned for minimal, moderate, and strong staining, respectively. The H-score was then calculated as 1 x %minimal+ 2 x %moderate+ 3 x %strong.

3.5. Cytokine Analysis

Twelve weeks post-intervention, nocturnal fasting and subsequent anesthesia were applied to rodent subjects. Three or four rats were randomly selected for blood collection from the left ventricle.

 doi:10.20944/preprints202412.0473.v1

The biochemical values of TC, TG, HDL-C, LDL-C, and liver enzymes AST and ALT were evaluated using Jiancheng Bio kits. The serum cytokine levels of TNF-α, IL-1β, IL-6, IL-10, and IL-17 were quantified by ELISA from Bio-Swamp (Wuhan, Hubei, China) in accordance with the specified protocol. Absorption readings at 450 nm were obtained using a MK3 microplate reader from LabSystems (Vantaa, Tiolitie, Finland).

3.6. Intestinal Microbiota Sequencing Procedure

Intestinal genomic DNA was isolated using Qiagen's DNeasy PowerSoil Kit and evaluated with Nanodrop ND-1000. Conventional agarose gel electrophoresis was employed for further verification. The V3-V4 region of the 16S RNA gene was amplified by 338F and 806R primers. Amplified products were purified with Agencourt AMPure beads and quantified by PicoGreen. The MiSeq platform generated up to 2×300 bp sequences per sample using Personalbio's MiSeq Reagent Kit v3. After quality control, sequences with 97% similarity formed operational taxonomic units (OTUs). Analyses focused on α diversity (Chao1 and Shannon indices) and β diversity (PCAs). Visualization was assisted by PCoA plots in MEGA 6.13.1 and GraPhlAn 1.1.3. A Venn diagram in the R package (v4.2.3) illustrated shared and unique OTUs across samples/clusters.

3.7. Fecal Microbiota In vitro Fermentation

Three faecal samples from donor rats of HFD (FFM) or NHP80 (NFM) were collected under aseptic conditions. Diluted to 20% (w/w) with Dulbecco phosphate buffer, samples underwent 10,000 rpm homogenization for 1 min and filtration through aseptic gauze. According to the protocol by Bianchi et al. [38], a 1.0 L medium was prepared, which contained 5.0 g each of soluble starch, peptone, and tryptone; 4.5 g each of yeast extract, NaCl, and KCl; 4.0 g of mucin; 3.0 g of casein; 2.0 g of pectin; 2.0 g of arabinogalactan; 1.5 g of $NaHCO_3$; 1.0 g of guar; 0.8 g of L-cysteine HCl-H_2O; 0.69 g of $MgSO_4$-H_2O; 0.5 g of KH_2PO_4; 0.5 g of K_2HPO_4; 0.4 g of bile salt; 0.08 g of $CaCl_2$; 0.005 g of $FeSO_4$-$7H_2O$; 1.0 mL of Tween 80, and 4.0 mL of 0.025% resazurin solution. This medium was autoclaved at 121°C for 15 min before being distributed into sterile glass vessels. A ratio of 1.6 mL medium to 0.4 mL bacterial suspension was used. The mixture was transferred to an anaerobic LAI-3 incubator (Longyue Instrument Corp., Shanghai, China) for shaking culture at 37°C, humidity 75%, and a gas composition of CO_2 (80%), N_2 (10%), and H_2 (10%). The shaker operated horizontally at a speed of 250 rpm. All experiments were repeated thrice.

3.8. Measurement of pH and Gas Production

Fermentation was terminated by immersing in ice for 5 min. Centrifugation was then performed at 8,000 rpm for 15 min to efficiently isolate the supernatant. The pH of these product solutions was quantified using a pHS-3C pH meter (Leici, Shanghai, China) after centrifugation. For gas production measurement during fermentation, a 10 mL disposable syringe was used. The needle tip of the syringe was inserted into the tube through the rubber stopper at the upper end of the anaerobic tube. The height of the raised syringe piston was used to determine gas production during the fermentation process.

3.9. Determination of SCFAs Content

SCFAs quantification involved centrifugation at 8,000 rpm for 15 min followed by filtration with a 0.22 μm filter. Analysis was executed using the ISQ-LT GC-MS system (Thermo Fisher, Waltham, MA, USA) with a TG-WAX column (30 m × 0.25 mm × 0.25 μm). The initial column temperature was 140°C for 6 min and then increased to 160°C at 5°C/min for another 6 min. Auxiliary injection and MS source temperatures were set at 180°C and 200°C respectively. Nitrogen flow rate was 0.8 mL/min, with an injection volume of 1 μL (split ratio of 20:1). Individual SCFA levels were derived from corresponding standard curves.

3.10. RT-qPCR Detection of Specific Bacterial Groups

Total RNA was isolated using Ambion TRIzol reagent (Cat#: 15596026, Foster City, CA, USA). Subsequently, cDNA conversion was performed with a Clontech Advantage RT-PCR Kit (Cat#:

 doi:10.20944/preprints202412.0473.v1

639505, Palo Alto, CA, USA). Real-time qPCR reactions were performed with Kapa Biosystems SYBR Green Master Mix (Cat#: KM4101, Wilmington, MA, USA) on a Bio-Rad real-time PCR system (Hercules, CA, USA) for 39 cycles. Primers for RT-PCR (sequences provided in Table 1) were custom-synthesized by GenScript Biotech Corp (Nanjing, Jiangsu, China). Bacterial abundance was normalized against total bacterial counts.

Table 1. Primer sequence information.

	Forward (5'-3')	Reverse (5'-3')
Total bacteria	TCCTACGGGAGGCAGCAGTGE	TTACCGCGGCTGCTGGCACG
Prevotella	CGGTGAATACGTTCYCGG	GGWTACCTTGTTACGACTT
Bacteroides	GGTGTCGGCTTAAGTGCCAT	GCATTYCACCGCTACACATG
Lactobacillus	GCAGCAGTAGGGAATCTTCCA	GCATTYCACCGCTACACATG
Clostridium	AGAGTTTGATCCTGGCTCAG	ACGGCTACCTTGTTACGACTT
Blautia producta	AGCTGACGACCTGATCGAGT	TCTCGAGCTGGTACGCTTCA

3.11. Western Blot Analysis

Total tissue protein from the colon was extracted by RIPA lysate and assayed by BCA protocol. Proteins were subjected to electrophoresis and then transferred to membranes. Subsequently, the membranes were blocked with 5% skim milk powder for one hour. Overnight incubation at 4°C with primary antibodies was carried out, followed by three washes with TBST. A secondary antibody dilution of 1:5,000 was added for one hour, followed by additional TBST washes. After adding a luminescent liquid, the membranes were imaged by a gel imaging system. Protein expression levels were assessed using Image J 1.8.0 software.

3.12. Statistical Methods

Statistical evaluations and figure generation were performed using Prism 8.0 (GraphPad, La Jolla, CA, USA). For specific tasks, one-way analysis of variance (ANOVA) with Tukey post hoc analysis or Student t-test was employed. Post hoc tests were utilized for significant overall effects (two-way or one-way). All statistical computations were carried out using SPSS Statistics 30. Significance threshold defined as $p < 0.05$.

4. Conclusions

NHP has shown substantial efficacy in fighting HFD-induced inflammation by modulating gut microbiome composition. Specifically, it influences Firmicutes ratios and promotes the growth of beneficial species such as *Bacteroides*, *Blautia*, *Lactobacillus*, and *Akkermansia*. These adjustments mainly resulted in increased production of SCFAs. In conclusion, NHP has demonstrated significant efficacy in alleviating HFD-induced inflammation by modulating gut microbiota composition and promoting SCFAs synthesis. These findings suggest that NHP may have potential as a therapeutic agent for the prevention and treatment of HFD-related diseases. Future studies should focus on translating these results into clinical applications and exploring the optimal dosage and treatment duration.

Author Contributions: K. L., Y. Z. and S. S.: Conceptualization, methodology, Formal analysis, validation, writing - original draft; G. Y.: Resources, software, Investigation, project administration, Supervision, project administration, writing - review & editing.

Acknowledgments: This research work was supported by the Grants from the Hunan Natural Science Foundation Project (2021JJ 31154).

Conflicts of Interest: The authors declare no conflict of interest.

 doi:10.20944/preprints202412.0473.v1

References

1. Ren, Q.; Sun, Q.; Fu, J. Dysfunction of autophagy in high-fat diet-induced non-alcoholic fatty liver disease. *Autophagy* **2024**, *20*, 221–241. https://doi.org/10.1080/15548627.2023.2254191.
2. He, X.; Gao, X.; Hong, Y.; Zhong, J.; Li, Y.; Zhu, W.; Ma, J.; Huang, W.; Li, Y.; Li, Y.; et al. High Fat Diet and High Sucrose Intake Divergently Induce Dysregulation of Glucose Homeostasis through Distinct Gut Microbiota-Derived Bile Acid Metabolism in Mice. *Journal of agricultural and food chemistry* **2024**, *72*, 230–244. https://doi.org/10.1021/acs.jafc.3c02909.
3. Hamamah, S.; Iatcu, O.C.; Covasa, M. Nutrition at the Intersection between Gut Microbiota Eubiosis and Effective Management of Type 2 Diabetes. *Nutrients* **2024**, *16*. https://doi.org/10.3390/nu16020269.
4. Le Chatelier, E.; Nielsen, T.; Qin, J.; Prifti, E.; Hildebrand, F.; Falony, G.; Almeida, M.; Arumugam, M.; Batto, J.M.; Kennedy, S.; et al. Richness of human gut microbiome correlates with metabolic markers. *Nature* **2013**, *500*, 541–546. https://doi.org/10.1038/nature12506.
5. Wu, J.; Zhao, Y.; Wang, X.; Kong, L.; Johnston, L.J.; Lu, L.; Ma, X. Dietary nutrients shape gut microbes and intestinal mucosa via epigenetic modifications. *Critical reviews in food science and nutrition* **2022**, *62*, 783–797. https://doi.org/10.1080/10408398.2020.1828813.
6. Yang, Q.; Cai, X.; Zhu, Y.; Hu, Z.; Wei, Y.; Dang, Q.; Zhang, Y.; Zhao, X.; Jiang, X.; Yu, H. Oat β-glucan supplementation pre- and during pregnancy alleviates fetal intestinal immunity development damaged by gestational diabetes in rats. *Food & function* **2023**, *14*, 8453–8466. https://doi.org/10.1039/d3fo00429e.
7. Yan, W.; Luo, J.; Yu, Z.; Xu, B. A critical review on intestinal mucosal barrier protection effects of dietary polysaccharides. *Food & function* **2024**, *15*, 481–492. https://doi.org/10.1039/d3fo03412g.
8. Gustafsson, J.K.; Johansson, M.E.V. The role of goblet cells and mucus in intestinal homeostasis. *Nature reviews. Gastroenterology & hepatology* **2022**, *19*, 785–803. https://doi.org/10.1038/s41575-022-00675-x.
9. Rana, N.; Privitera, G.; Kondolf, H.C.; Bulek, K.; Lechuga, S.; De Salvo, C.; Corridoni, D.; Antanaviciute, A.; Maywald, R.L.; Hurtado, A.M.; et al. GSDMB is increased in IBD and regulates epithelial restitution/repair independent of pyroptosis. *Cell* **2022**, *185*, 283–298.e217. https://doi.org/10.1016/j.cell.2021.12.024.
10. Dolinger, M.; Torres, J.; Vermeire, S. Crohn's disease. *Lancet (London, England)* **2024**, *403*, 1177–1191. https://doi.org/10.1016/s0140-6736(23)02586-2.
11. Fan, B.; Zhou, J.; Zhao, Y.; Zhu, X.; Zhu, M.; Peng, Q.; Li, J.; Chang, X.; Shi, D.; Yin, J.; et al. Identification of Cell Types and Transcriptome Landscapes of Porcine Epidemic Diarrhea Virus-Infected Porcine Small Intestine Using Single-Cell RNA Sequencing. *Journal of immunology (Baltimore, Md. : 1950)* **2023**, *210*, 271–282. https://doi.org/10.4049/jimmunol.2101216.
12. Hsu, H.P.; Lai, M.D.; Lee, J.C.; Yen, M.C.; Weng, T.Y.; Chen, W.C.; Fang, J.H.; Chen, Y.L. Mucin 2 silencing promotes colon cancer metastasis through interleukin-6 signaling. *Sci Rep* **2017**, *7*, 5823. https://doi.org/10.1038/s41598-017-04952-7.
13. Yao, D.; Dai, W.; Dong, M.; Dai, C.; Wu, S. MUC2 and related bacterial factors: Therapeutic targets for ulcerative colitis. *EBioMedicine* **2021**, *74*, 103751. https://doi.org/10.1016/j.ebiom.2021.103751.
14. Dong, S.; Wu, S.; Li, L.; Hao, F.; Wu, J.; Liao, Z.; Wang, J.; Zhong, R.; Wei, H.; Fang, X. Alleviation of lipid metabolic dysfunction through regulation of intestinal bacteriophages and bacteria by green tea polyphenols in Ob/Ob mice. *Food Chem* **2024**, *456*, 139988. https://doi.org/10.1016/j.foodchem.2024.139988.
15. Yang, W.; Yu, T.; Huang, X.; Bilotta, A.J.; Xu, L.; Lu, Y.; Sun, J.; Pan, F.; Zhou, J.; Zhang, W.; et al. Intestinal microbiota-derived short-chain fatty acids regulation of immune cell IL-22 production and gut immunity. *Nat Commun* **2020**, *11*, 4457. https://doi.org/10.1038/s41467-020-18262-6.
16. Wang, M.; Zhao, H.; Wen, X.; Ho, C.T.; Li, S. Citrus flavonoids and the intestinal barrier: Interactions and effects. *Compr Rev Food Sci Food Saf* **2021**, *20*, 225–251. https://doi.org/10.1111/1541-4337.12652.
17. Dai, H.; Jiang, Y.; Liu, S.; Li, D.; Zhang, X. Dietary flavonoids modulate the gut microbiota: A new perspective on improving autism spectrum disorder through the gut-brain axis. *Food Research International* **2024**, *186*, 114404.
18. Ortiz, A.C.; Fideles, S.O.M.; Reis, C.H.B.; Bellini, M.Z.; Pereira, E.; Pilon, J.P.G.; de Marchi, M.; Detregiachi, C.R.P.; Flato, U.A.P.; Trazzi, B.F.M.; et al. Therapeutic Effects of Citrus Flavonoids Neohesperidin, Hesperidin and Its Aglycone, Hesperetin on Bone Health. *Biomolecules* **2022**, *12*. https://doi.org/10.3390/biom12050626.
19. Li, J.; Rui, X.; Xu, L.; Liu, Y.; Yang, Y.; Yin, D. Enhanced therapeutic effect on colitis with powder formulations of Painong San associated with the promotion of intestinal adhesion and absorption. *Journal of ethnopharmacology* **2022**, *289*, 115030. https://doi.org/10.1016/j.jep.2022.115030.
20. Chen, S.Y.; Zhou, Q.Y.; Chen, L.; Liao, X.; Li, R.; Xie, T. The Aurantii Fructus Immaturus flavonoid extract alleviates inflammation and modulate gut microbiota in DSS-induced colitis mice. *Frontiers in nutrition* **2022**, *9*, 1013899. https://doi.org/10.3389/fnut.2022.1013899.
21. Kirschner, N.; Poetzl, C.; von den Driesch, P.; Wladykowski, E.; Moll, I.; Behne, M.J.; Brandner, J.M. Alteration of tight junction proteins is an early event in psoriasis: putative involvement of proinflammatory cytokines. *Am J Pathol* **2009**, *175*, 1095–1106. https://doi.org/10.2353/ajpath.2009.080973.

22. Guzmán-Gómez, O.; García-Rodríguez, R.V.; Pérez-Gutierrez, S.; Rivero-Ramírez, N.L.; García-Martínez, Y.; Pablo-Pérez, S.S.; Pérez-Pastén-Borja, R.; Cristóbal-Luna, J.M.; Chamorro-Cevallos, G. Protective effect of the phycobiliproteins from arthrospira maxima on indomethacin-induced gastric ulcer in a rat model. *Plants* **2023**, *12*, 1586. https://doi.org/10.3390/plants12081586.
23. Tian, S.; Zhao, Y.; Qian, L.; Jiang, S.; Tang, Y.; Han, T. DHA-enriched phosphatidylserine alleviates high fat diet-induced jejunum injury in mice by modulating gut microbiota. *Food & function* **2023**, *14*, 1415–1429. https://doi.org/10.1039/d2fo03019e.
24. Yang, J.; Martínez, I.; Walter, J.; Keshavarzian, A.; Rose, D.J. In vitro characterization of the impact of selected dietary fibers on fecal microbiota composition and short chain fatty acid production. *Anaerobe* **2013**, *23*, 74–81.
25. Zhai, Z.; Yang, Y.; Chen, S.; Wu, Z. Long-Term Exposure to Polystyrene Microspheres and High-Fat Diet-Induced Obesity in Mice: Evaluating a Role for Microbiota Dysbiosis. *Environ Health Perspect* **2024**, *132*, 97002. https://doi.org/10.1289/ehp13913.
26. Gao, Z.; Yin, J.; Zhang, J.; Ward, R.E.; Martin, R.J.; Lefevre, M.; Cefalu, W.T.; Ye, J. Butyrate Improves Insulin Sensitivity and Increases Energy Expenditure in Mice. *Diabetes* **2009**, *58*, 1509–1517. https://doi.org/10.2337/db08-1637.
27. Al-Lahham, S.; Roelofsen, H.; Rezaee, F.; Weening, D.; Hoek, A.; Vonk, R.; Venema, K. Propionic acid affects immune status and metabolism in adipose tissue from overweight subjects. *Eur J Clin Invest* **2012**, *42*, 357–364. https://doi.org/10.1111/j.1365-2362.2011.02590.x.
28. Magne, F.; Gotteland, M.; Gauthier, L.; Zazueta, A.; Pesoa, S.; Navarrete, P.; Balamurugan, R. The Firmicutes/Bacteroidetes Ratio: A Relevant Marker of Gut Dysbiosis in Obese Patients? *Nutrients* **2020**, *12*. https://doi.org/10.3390/nu12051474.
29. Lau, H.C.; Zhang, X.; Ji, F.; Lin, Y.; Liang, W.; Li, Q.; Chen, D.; Fong, W.; Kang, X.; Liu, W.; et al. Lactobacillus acidophilus suppresses non-alcoholic fatty liver disease-associated hepatocellular carcinoma through producing valeric acid. *EBioMedicine* **2024**, *100*, 104952. https://doi.org/10.1016/j.ebiom.2023.104952.
30. Hosomi, K.; Saito, M.; Park, J.; Murakami, H.; Shibata, N.; Ando, M.; Nagatake, T.; Konishi, K.; Ohno, H.; Tanisawa, K.; et al. Oral administration of Blautia wexlerae ameliorates obesity and type 2 diabetes via metabolic remodeling of the gut microbiota. *Nature communications* **2022**, *13*, 4477. https://doi.org/10.1038/s41467-022-32015-7.
31. Liu, X.; Mao, B.; Gu, J.; Wu, J.; Cui, S.; Wang, G.; Zhao, J.; Zhang, H.; Chen, W. Blautia-a new functional genus with potential probiotic properties? *Gut microbes* **2021**, *13*, 1–21. https://doi.org/10.1080/19490976.2021.1875796.
32. Zhang, T.; Li, Q.; Cheng, L.; Buch, H.; Zhang, F. Akkermansia muciniphila is a promising probiotic. *Microb Biotechnol* **2019**, *12*, 1109–1125. https://doi.org/10.1111/1751-7915.13410.
33. Gullón, B.; Gullón, P.; Tavaria, F.; Pintado, M.; Gomes, A.M.; Alonso, J.L.; Parajó, J.C. Structural features and assessment of prebiotic activity of refined arabinoxylooligosaccharides from wheat bran. *Journal of Functional Foods* **2014**, *6*, 438–449.
34. Kaur, A.; Rose, D.J.; Rumpagaporn, P.; Patterson, J.A.; Hamaker, B.R. In vitro batch fecal fermentation comparison of gas and short-chain fatty acid production using "slowly fermentable" dietary fibers. *J Food Sci* **2011**, *76*, H137–H142. https://doi.org/10.1111/j.1750-3841.2011.02172.x.
35. Li, Z.; Liang, H.; Hu, Y.; Lu, L.; Zheng, C.; Fan, Y.; Wu, B.; Zou, T.; Luo, X.; Zhang, X.; et al. Gut bacterial profiles in Parkinson's disease: A systematic review. *CNS Neurosci Ther* **2023**, *29*, 140–157. https://doi.org/10.1111/cns.13990.
36. Li, S.; Liu, W.; Li, Y.; Che, X.; Xiao, P.; Liu, S.; Ma, Y.; Ren, D.; Wu, L.; Wang, Q.; et al. Extraction, purification, structural characterization and anti-hyperlipidemia activity of fucoidan from Laminaria digitata. *International journal of biological macromolecules* **2024**, *279*, 135223. https://doi.org/10.1016/j.ijbiomac.2024.135223.
37. Küçükgöz, K.; Venema, K.; Trząskowska, M. Gut microbiota modulatory capacity of fermented ketchup in a validated in vitro model of the colon. *Food research international (Ottawa, Ont.)* **2024**, *192*, 114801. https://doi.org/10.1016/j.foodres.2024.114801.
38. Bianchi, F.; Dall'Asta, M.; Del Rio, D.; Mangia, A.; Musci, M.; Scazzina, F. Development of a headspace solid-phase microextraction gas chromatography–mass spectrometric method for the determination of short-chain fatty acids from intestinal fermentation. *Food Chemistry* **2011**, *129*, 200–205.